The Application of Wavelets to Measured Equation of Invariance

Byungje Lee, Youngki Cho, and Jaemin Lee

Abstract

The measured equation of invariance (MEI) method was introduced as a way to determine the electromagnetic fields scattered from discrete objects. Unlike more traditional numerical methods, MEI method gives local equations and sparse matrices. Therefore, the savings in storage and computing time by the MEI method over conventional methods are very substantial. In this work, Haar wavelets are applied to the measured equation of invariance (MEI) to solve two-dimensional scattering problem. We refer to "MEI method with wavelets" as "Wavelet MEI method." The proposed method leads to a significant saving in the CPU time compared to the MEI method that does not use wavelets as metrons. The results presented in this work promise that the Wavelet MEI method can give an accurate result quickly. We believe it is the first time that wavelets have been applied in conjunction with the MEI method to solve this scattering problem.

I. Introduction

The MEI method, first proposed by K. K. Mei in 1992 [1], is a technique that can be used to terminate a finite difference (FD) mesh arbitrarily close to the object of interest, avoiding the use of absorbing boundary conditions, which require the mesh to extend beyond the region of interest, with increase in computation time and storage memory. Initially, it was applied to two-dimensional conducting objects. Subsequently, it was applied to a broader class of problems [2]-[6]. Since the MEI method still preserves the sparsity of finite difference equations, it results in dramatic savings in computing time and memory needs. As discussed in [2], the time required to fill the matrix in the MEI method is roughly $O(N^2)$, where N is the number of unknowns on the boundary. Since the matrix is sparse, the time required to invert the matrix is small (O(N)). Thus the total computation time of this method is dominated by the time required to fill the matrix obtained by the integration process. This is in contrast to the traditional method of moments (MoM) approach in which the time required for the integration process to fill the matrix is also $O(N^2)$, but since the method leads to a fully dense matrix, the time required for the inversion is $O(N^3)$.

Since the MEI method spends most of the CPU time on integration process to fill the matrix, the efficiency of the method can be improved by accelerating the integration process. For this reason, the integration with transform techniques or variable step routines was suggested in [2]. In this work, we propose a wavelet transform based technique to further improve the computational efficiency of the MEI method. The first paper on compactly supported orthonormal wavelets appeared only 9 years ago [7]. Since then, wavelets have been applied to solve a large class of problems in various fields of mathematics, science, and engineering. The wavelets are generated using dilation and translation of a basis function. The properties and applications of wavelets have been investigated extensively in [8], [9]. Wavelets have been used to develop fast numerical algorithms in various fields [10], [11]. Wavelets have also been used in many electromagnetic applications [12]-[15]. Considering the success of wavelets in various fields their application in conjunction with the MEI method to electromagnetic field problems is timely. The MEI method requires selection of a set of metrons. In this paper, We will use compactly supported orthogonal Haar wavelets as metrons.

Manuscript received September 2, 1997; accepted April 8, 1998.
Byungje Lee is with the Department of Radio Science & Engineering, Kwangwwoon University.
Youngki Cho is with the Electrical Engineering Kyungpook National University.
Jaemin Lee is with the Telecommunication Development Center Information & System Business Samsung Electronics Co., Ltd.

II. Review of the Mei Method

In electromagnetic boundary-value problems, the governing differential equation is usually the Helmoltz equation:

$$(\nabla^2+k^2)\Phi(\bar{\gamma})=0 \tag{1}$$

where k is the wavenumber. The solution of the Helmoltz equation may be approached by an integral equation or a differential equation formulation. In two-dimensional scattering from a conducting object, the integral solution to equation (1) can be expressed in terms of a source $J(\bar{\gamma}')$ on the object boundary

$$\Phi(\bar{\gamma})=\int G(\bar{\gamma})\mid(\bar{\gamma}')J(\bar{\gamma})dc' \tag{2}$$

where $\Phi(\bar{\gamma})$ is the scattered field, $G(\bar{\gamma}\mid\bar{\gamma}')$ is the Green's function in free space and c is the contour of the conducting object. Equation (2) is an integral equation with unknown $J(\bar{\gamma}')$ and can be solved by the MoM. In the MoM approach, the computation domain is limited in the exactly interested region (object boundary).

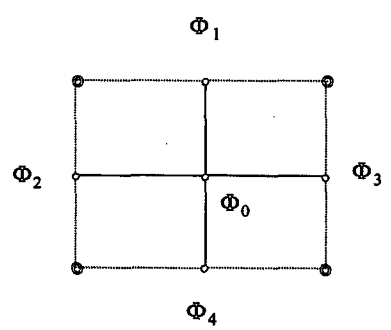

Fig. 1. The five nodes in the computational mesh.

It is important that we recognize the fact that MoM is limited in application to radiation and scattering from objects that are electrically large. This is because that the cost of storing, inverting, and computing matrix elements becomes prohibitively large. If the solution region is divided into a uniform mesh and a local configuration of nodes as shown in Fig. 1, equation(1) can be approximated using central difference to obtain

$$\Phi_1+\Phi_2+(k^2\triangle^2-4)\Phi_0+\Phi_3+\Phi_4=0 \tag{3}$$

where $\triangle$ is the separation between mesh points. This finite difference (FD) equation is invariant to the location in space, to the geometry of the problem, and the field of excitation. From equation (3), we notice that only nearest neighboring nodes affect the value of at each node. Hence application of equation (3) to all free nodes in the solution region results a set of simultaneous equation of the form

$$[A][\Phi]=[B] \tag{4}$$

where [A] is a sparse matrix(it has many zero elements), $[\Phi]$ is a column matrix consisting of the unknown values at the free nodes, and [B] is a column matrix containing the known values at the fixed nodes. In contrast to the MoM, equation (4) can be solved relatively rapidly in terms of time per unknown. Even though the sparsity is the appeal of the FD method, finite difference meshes expend to some distance away from the region of interest, which makes the size of equation (4) very large. There is also no simple way to terminate the computational mesh with reasonable accuracy for unbounded problems. The ideal case would be to find a set of equations limited to a small domain and still held the sparsity of the matrix. The MEI method combines features of both differential and integral based methods. Equation (3) can be written more generally as

$$\sum_{i=0}^{NN}a_i\Phi_i=0 \tag{5}$$

where NN is the number of nodes and the a_i's represent appropriate weights. Basically, the MEI method provides a mean to select appropriate a_i's in equation (5) so that the mesh need not be orthogonal. Thus, this allows the fields at the nodes on the edge of the computational domain to be related simply to points on the interior. Fig. 2 shows typical configuration of nodes at the edge of the computational mesh. Furthermore, MEI method maintains that equation (5) is local dependent, geometry specific, and invariant to the field of excitation. To illustrate the technique, consider the configuration of the nodes (NN=3) shown in Fig. 2(a). One seeks a_i's such that

$$\sum_{i=0}^{NN=3}a_i\Phi_i=0 \tag{6}$$

Since equation (6) is a homogeneous equation, one of the weights (e.g., a_0) may be chosen arbitrarily. The remaining three weights are determined via three equations. These equations are obtained by using the measuring functions. In the MEI method, the measuring functions are derived from the metrons using equation (2)

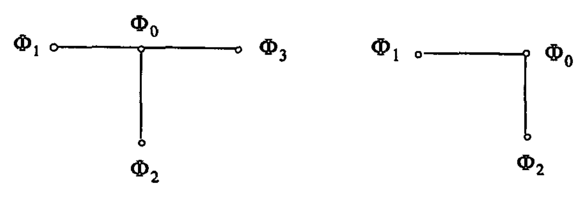

Fig. 2. Geometry of nodes at the edge of the computational mesh.

$$\Phi^k(\bar{\gamma})=\int_c G(\bar{\gamma}\mid\bar{\gamma}')J_k(\bar{\gamma}')dc' \tag{7}$$

where the current densities $J_k(\bar{\gamma}')$, k=1,2, ..., M, are named the metrons, and Φ^k are named the measuring functions. It is noticed that each metron gives rise to the measuring function and is not used to present the solutions. $J_k(\bar{\gamma}')$ provides the equation with information about the geometry of the object, and $G(\bar{\gamma} \mid \bar{\gamma}')$ provides the information about the differential operator and the exterior boundary conditions. Φ^k is not the specific solution we are looking for, but, it may be the scattered field of some unknown incident field. In the MoM, the unknown current $J_k(\bar{\gamma}')$ should be expanded to solve equation (2) with known basis function on the surface of the object because the accuracy of the MoM depends on the ability of the basis functions. Since equation (7) was derived by using equation (2), one may think that the metrons $J_k(\bar{\gamma}')$ in equation (7) are also used to represent an approximation to the exact current distribution. This is not true because the MEI method suggests that the calculated solution is represented not by a linear combination of metrons, representing an expansion of the current distribution, but rather by a linear combination of measuring solutions, representing an expansion of the scattered field at the mesh edges. Assuming $a_0=1$, the remaining *NN* coefficients in equation (6) can be solved from a system of M simultaneous equations as

$$\begin{bmatrix} a_1 \\ a_2 \\ a_3 \end{bmatrix} = -\begin{bmatrix} \Phi_1^1 & \Phi_2^1 & \Phi_3^1 \\ \Phi_1^2 & \Phi_2^2 & \Phi_3^2 \\ \Phi_1^3 & \Phi_2^3 & \Phi_3^3 \end{bmatrix}^{-1} \cdot \begin{bmatrix} \Phi_0^1 \\ \Phi_0^2 \\ \Phi_0^3 \end{bmatrix} \tag{8}$$

which can be written as

$$[a] = -[F]^{-1}[F_0] \tag{9}$$

where [*F*] contains the measured fields at the neighboring nodes while [F_0] contains the fields sampled at the zeroth node. One may wish to more metrons than unknown. In this case (M>*NN*), the coefficients are obtained through least squares.

III. Wavelet Mei Method

The accuracy of the MEI method depends on the ability of the measuring functions to approximate the field at the boundary, not on the ability of the metrons to approximate the source [5]. Therefore, there exists a wide variety of functions, which can be used as metrons. The choice of metrons in [1] and [16] was

$$J_k = \begin{cases} \cos\dfrac{2k\pi l}{L}, & k=0,1,2 \\ \sin\dfrac{2k\pi l}{L}, & k=1,2 \end{cases} \tag{10}$$

where *L* is the perimeter length of the object, and *l* is the length along the perimeter $(0 \le l/L \le 1)$.

In this work, Haar wavelets are used to improve the computational efficiency of the MEI method. Where Haar wavelets are used as metrons, (7) becomes

$$\Phi^k(\bar{\gamma}) = \int_c G(\bar{\gamma} \mid \bar{\gamma}') h_k(\bar{\gamma}') dc' \tag{11}$$

where are the Haar wavelet coefficients and are the Haar wavelets as follows:

$$h_0(\bar{\gamma}') = \begin{cases} 1 & \text{if } 0 < \bar{\gamma}' < 1, \\ 0 & \text{otherwise} \end{cases} \tag{12}$$

and for, $i \ge 0,\ 0 \le j \le 2^{i}$, and $k = 2^i + j$,

$$h_k(\bar{\gamma}') = h_{i,j}(\bar{\gamma}') = \begin{cases} 2^{i/2} & \text{if } 2^i j < 2^{-i}(j+1/2) \\ -2^{i/2} & \text{if } 2^{-i}(j+1/2) < \bar{\gamma}' < (j+1) \\ 0 & \text{other} \end{cases} \tag{13}$$

In fact, the Haar wavelet coefficients in (11) and the measuring functions in (7) are equal. Since Haar wavelets are orthogonal, we can use the pyramid scheme to calculate the Haar coefficients [17]. An important aspect of the pyramid scheme is that it is a fast algorithm. Thus, calculating the complete set of the Haar wavelet coefficients with *N* average values requires 2(*N*-1) additions and *N* multiplications. Given $N=2^n$ samples of a function, which can be thought of as values of scaled averages

$$S_k^0 = 2^{n/2} \int_{2^{-n}(k-1)}^{2^{-n}k} f(x)dx, \tag{14}$$

of f on intervals of length 2^{-n}, one may get the Haar coefficients

$$d_k^1 = \frac{1}{\sqrt{2}}(s_{2k-1}^0 - s_{2k}^0) \tag{15}$$

and averages

$$s_k^1 = \frac{1}{\sqrt{2}}(s_{2k-1}^0 + s_{2k}^0) \tag{16}$$

on the interval of length 2^{-n+1}. By repeating the above procedure, one may obtain the Haar coefficients and averages

$$d_k^{j+1} = \frac{1}{\sqrt{2}}(s_{2k-1}^j - s_{2k}^j) \tag{17}$$

$$s_k^{j+1} = \frac{1}{\sqrt{2}}(s_{2k-1}^j + s_{2k}^j) \tag{18}$$

for j = 0, 1, ..., n-1 and k = 1, 2, ..., 2^{n-j-1}. An important aspect of the whole decomposition is that it is a fast algorithm. If we start *N* samples s_k^0, then we should calculate *N/2* averages s_k^1, and *N/2* differences d_k^1; from the averages s_k^1 we obtain *N/4* averages s_k^2 and *N/4* differences d_k^2, etc. Now, we will demonstrate the procedure for obtaining measuring functions by using the integral wavelet transform. Here, we use only eight samples $a_1, a_2, a_3, a_4, a_5, a_6, a_7, a_8$ which can be thought of as values of scaled averages in intervals of length 1/8 of a function defined on [0, 1]. Then, the first calculation involved is

$$s_1=\frac{1}{\sqrt{2}}(a_1+a_2),\quad s_2=\frac{1}{\sqrt{2}}(a_3+a_4)$$
$$s_3=\frac{1}{\sqrt{2}}(a_5+a_6),\quad s_4=\frac{1}{\sqrt{2}}(a_7+a_8) \tag{19}$$

$$d_1=\frac{1}{\sqrt{2}}(a_1-a_2),\quad d_2=\frac{1}{\sqrt{2}}(a_3-a_4)$$
$$d_3=\frac{1}{\sqrt{2}}(a_5-a_6),\quad d_4=\frac{1}{\sqrt{2}}(a_7-a_8) \tag{20}$$

In the second stage, discarding d_1, d_2, d_3, and d_4, we consider sums s_1, s_2, s_3, and s_4, as new samples which are averages on intervals of length 1/4:

$$ss_1=\frac{1}{\sqrt{2}}(s_1+s_2),\quad ss_2=\frac{1}{\sqrt{2}}(s_3+s_4)$$
$$ds_1=\frac{1}{\sqrt{2}}(s_1-s_2),\quad ds_2=\frac{1}{\sqrt{2}}(s_3-s_4) \tag{21}$$

By repeating this procedure, one may compute sum of sums sss_1, and difference of sums dss_2 as shown in Fig. 3.

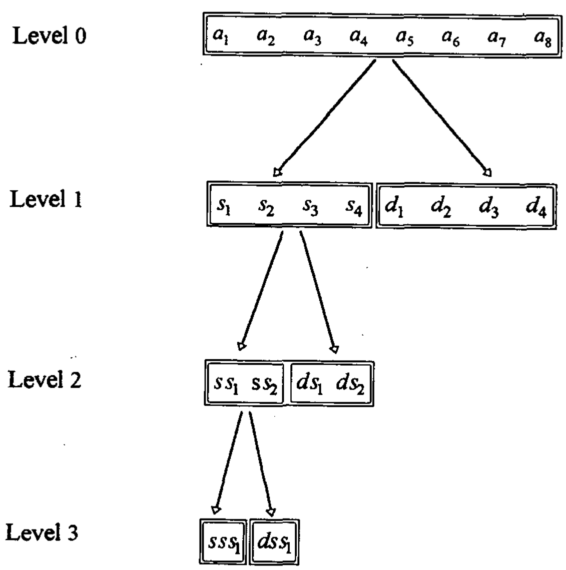

Fig. 3. The pyramid scheme for calculating the Haar wavelet coefficients.

The measuring functions Φ^k, $k = 1, 2, ..., 8$, in equation (11) are obtained by choosing the second block in each low and the first and second entry on the last row in Fig. 3:

$$\begin{aligned} \Phi^1&=sss_1, & \Phi^5&=d_1 \\ \Phi^2&=dss_1, & \Phi^6&=d_2 \\ \Phi^3&=ds_1, & \Phi^7&=d_3 \\ \Phi^4&=ds_2, & \Phi^8&=d_4 \end{aligned} \tag{22}$$

One may also draw the Haar wavelets which correspond to the entries in the rectangle. Fig. 4 displays the Haar wavelets corresponding the Haar wavelet coefficients.

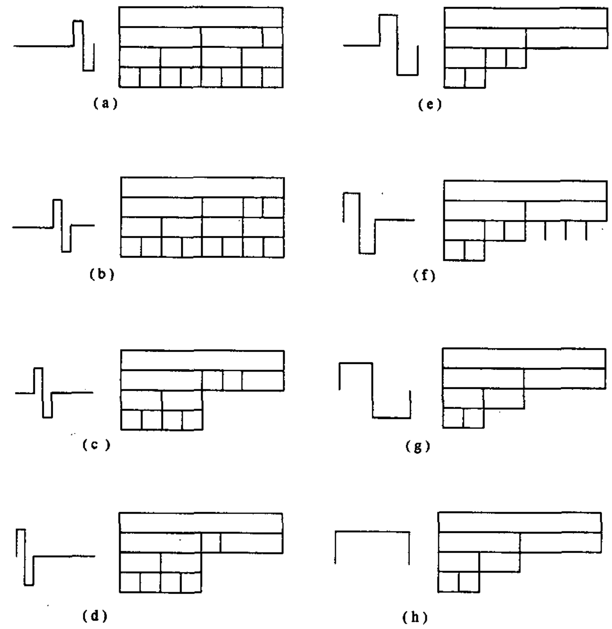

Fig. 4. The first Haar wavelets correspond to the entries in the rectangle.

IV. Numerical Result and Discussion

In this work, the MEI and the Wavelet MEI methods were applied to solve the scattering problem of two-dimensional conducting cylinders as shown in Fig. 5 for E-wave and H-wave incidences ($\varphi^i=0$), and the MoM solutions were obtained to validate the results of the two methods. For all figures, N is the number of unknown, M is the number of metrons, and NL is the number of mesh layers.

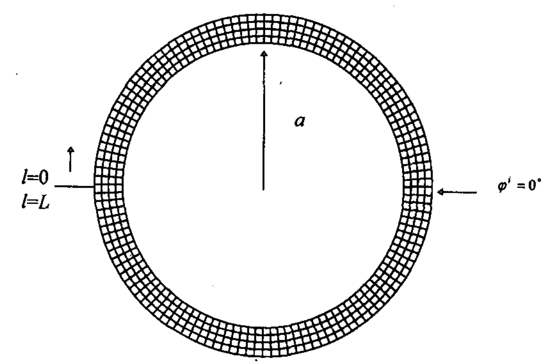

Fig. 5. Cylinder and the mesh around it.

In Fig. 6 and Fig. 7, the induced electric currents on the surface of a circular cylinder obtained by the MEI and the

Wavelet MEI methods are compared with those computed by the MoM, respectively. In Fig. 6, sine and cosine functions in equation (10) are used as metrons.

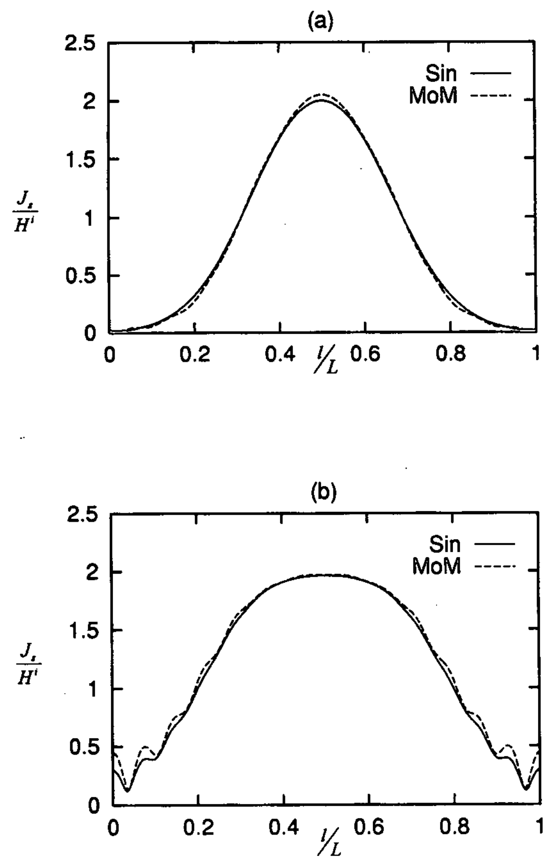

Fig. 6. Induced current on the surface of the circular cylinder for as calculated by MEI and MoM for (a) E-wave, (b) H-wave. N =1024, M =8, NL =10, Metron used: 1, sin, cos

Haar wavelets in equation (12) and (13) are used as metrons in Fig. 7. For the MoM, the pulse functions are used as basis in both Fig. 6 and Fig. 7. One may see that there is an excellent agreement among the three different methods. Fig. 8 shows the CPU times required to obtain solutions with increasing number of unknowns (N) for the four methods. Keeping the electric size of object N is increased by reducing the step size on the object and at the mesh edge. We also observe excellent agreement over a wide frequency range (α = 0.01 λ, 0.1 λ, 1 λ, 10 λ, 100 λ). As mentioned in Section I, the integration process of the MEI method is of order $O(N^2)$ and the dominant part of the calculation. In the MoM, the integration process to fill the matrix is also $O(N^3)$, but since the matrix is full the inversion is $O(N^3)$ and is the dominant part of the calculation. For low values of N, the dominant part is filling the matrix ($O(N^2)$), but as N increases, the inversion of the matrix ($O(N^3)$) starts to take over. Since there is no way to solve a full-matrix equation in less than $O(N^3)$ time, there is very little incentive to speed up the integration process in the MoM, and this is why very little effort has been done in this direction. If one accelerate the integration process of the MEI, the computational efficiency of this method can be improved.

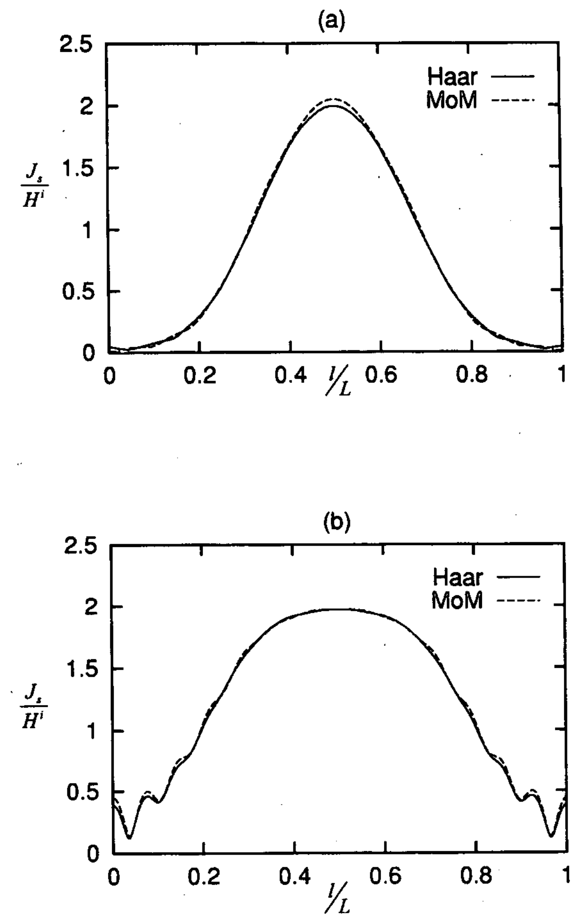

Fig. 7. Induced current on the surface of the circular cylinder foras calculated by Wavelet MEI and MoM for (a) E-wave, (b) H-wave. N =1024, M =8, NL =10, Metron used: Haar wavelets

Fig. 8, which is in the double logarithmic plot, shows that the CPU time of the MEI method can be significantly reduced by using the Haar wavelets. Generally, several metrons are required to calculate unknown surface current on a circular cylinder boundary. Thus, one may obtain Haar wavelet coefficients with a small number of scaled average values. In this case, these average values can be computed by using integration techniques. In this work, the integration was done by Gaussian quadrature using a ten-term formula. It is indicated that the Wavelet MEI method with a small number of scaled average values provides a solution much more quickly. A SUN Sparc 20 was used to check the CPU time of each method.

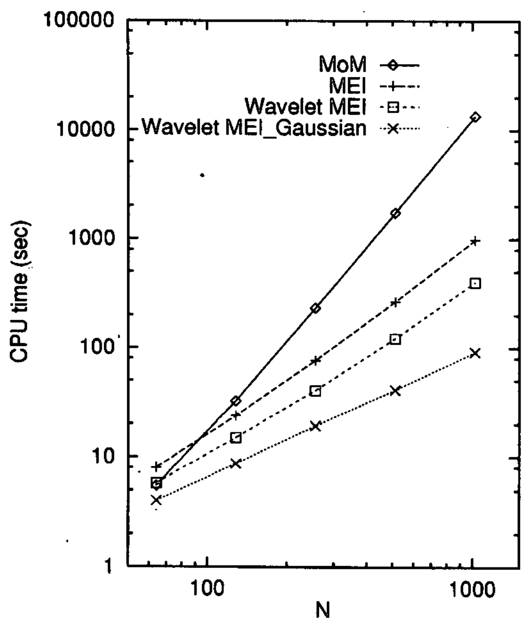

Fig. 8. Comparison of the CPU times with varying the number of unknowns. M =8, NL =10.

V. Conclusion

In this work, the significant saving of the computational time of the MEI method was achieved by using wavelets as metrons. The application of the MEI and the Wavelet MEI methods to a circular cylinder gives excellent results. The results were verified by the MoM which is very robust. However, as the perimeter of cylinder becomes large one may need to increase the number of mesh points to get accurate solutions. Increasing the number of mesh points requires more CPU time to obtain solution by the MEI method. In this case, the Wavelet MEI method makes the work very easy. The results presented in this work indicates that the Wavelet MEI method has the potential to provide an accurate solution much more quickly. When the MEI method applies to three-dimensional problems, the metron would be a function of two variables, rather than one. In this case, the Wavelet MEI method with two-dimensional wavelet transform will be a significant tool.

References

[1] K. K. Mei, R. Pous, Z. Chen, and Y. W. Liu, "The measured equation of invariance: A new concept in field computation," *IEEE AP-S International Symposium,* Chicago, Ill., pp. 2047-2050, July 1992.

[2] R. Pous, " The measured equation of invariance: A new concept in field computation," Ph.D. dissertation, University of California, Berkeley, CA, 1992.

[3] R. Pous, M. D. Prouty, and K. K. Mei, "Application of the measured equation of invariance to radiation and scattering by flat surfaces," *IEEE AP-S International Symposium,* Ann Arbor, Michigan, pp. 540, 1993.

[4] W. Hong, Y. W. Liu, and K. K. Mei, "Application of the measured equation of invariance to solve scattering problems involving a penetrable medium," *Radio Science,* vol. 29, pp. 879-906, July-August 1994.

[5] M. D. Prouty, "Application of the measured equation of invariance to planar microstrip structures," Ph.D. dissertation, University of California, Berkeley, 1994.

[6] Z. Chen, W. Hong, and W. X. Zhang, "Electromagnetic Scattering from a chiral cylinder-General case," *IEEE Trans. Antennas and Propagat.* vol. 44, pp. 912-917, July 1996.

[7] I. Daubechies, "Orthonormal bases of compactly supported wavelets," *Comm. Pure Appl. Math.,* vol. 41, pp. 909-996, 1988.

[8] L. L. Schumaker, *Recent Advances in Wavelet Analysis,* Boston, Academic Press, 1994.

[9] G. Kaiser, *A Friendly Guide to Wavelets,* Boston, Birkhauser, 1994.

[10] G. Beylkin, "On the representation of operators in bases of compactly supported wavelets," *SIAM J. Numer. Anal.* vol. 29, pp. 1716-1740, 1992.

[11] G. Beylkin, "Wavelet and fast numerical algorithms," Different Perspective on Wavelets, (I. Daubechies, ed.) American Mathematical Society), pp. 89-117, 1993.

[12] F. X. Canning and S. R. Laxpati, "Joint secession: new technique in computational electromagnetics," *IEEE AP-S international Symposium,* pp. 1131-1151, June 1993.

[13] C. K. Chui and A. K. Chan, "Special session M-AP1: wavelets in electromagnetics," *IEEE AP-S international Symposium,* pp. 1-36, June 1994.

[14] G. Wang, "A hybrid wavelet expansion and boundary element analysis of electromagnetic scattering from conduction objects," *IEEE Trans. Antennas and Propagat.* vol. 43, pp. 170-178, Feb. 1995.

[15] J. C. Goswami, A. K. Chan, and C. K. Chui, "On solving first-kind integral equations using wavelets on a bounded interval," *IEEE Trans. Antennas and Propagat.* vol. 43, pp. 614-622, June 1995.

[16] K. K. Mei, R. Pous, Z. Chen, Y. W. Liu, and M. D. Prouty, "Measured equation of invariance: a new concept in field computations," *IEEE Trans. Antennas and Propagat.* vol. 42, pp. 320-327, Mar. 1994.

[17] G. Beylkin, R. Coifman, and V. Rokhlin, "Fast wavelet transforms and numerical algorithms I," *Comm. Pure Appl. Math.* Vol. 44, pp. 141-183, 1991.

Byungje Lee received the B.S. degree in electronics engineering from Kyungpook National University, Taegu, Korea, in 1988, and the M.S. and Ph.D. Degrees in electrical Engineering from Southern Illinois University at Carbondale, Carbondale, IL, in 1994 and 1997, respectively. From 1991-1997, he was a Research and Teaching Assistant at Southern Illinois University. In 1997, he was employed as a senior researcher at the Telecommunication Research and Development Center, Samsung Electronics, where he worked in the area of antenna design for Wireless LAN, Wireless ATM. Since 1998, he has been an assistant professor of Department of Radio Science and Engineering at Kwangwoon University. His current research interests include microwave antennas and numerical methods in electromagnetics.

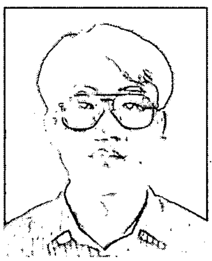

Jaemin Lee was born in Masan on September 24, 1959. He received the B.S. degree in Electronics Engineering from Kyungpook National University, Taegu, Korea in 1982 and the M.S. and Ph.D. degrees in Electrical Engineering from Korea Advanced Institute of Science and Technology, Seoul, in 1984 and 1989, respectively. He joined Samsung Electronics Research Center in 1988, where he developed Hand Held Phone, RF components, and MMIC for mobile communications. Now he is developing Imt2000 Hand Held Phone.

Youngki Cho was born in Seoul, Korea, on September 12, 1954. He received the B.S. degree in electronics engineering from the Seoul National University, Seoul, Korea, in 1978, and the M.S. and Ph.D. degree in electrical engineering from the Korea Advanced Institute of Science and Technology, Taejeon, Korea, in 1981 and 1998, respectively. Since 1981 he has been with Department of Electronics, Kyungpook National University, Taegu, Korea. His research interests are in the area of electromagnetic scattering, microwaves, optics, and antenna theory. Dr. Cho is a member of the Institute of Electrical and Electronics Engineers.